NASA/TM—2008-215176

Gas Foil Bearing Misalignment and Unbalance Effects

Samuel A. Howard
Glenn Research Center, Cleveland, Ohio

May 2008

NASA STI Program . . . in Profile

Since its founding, NASA has been dedicated to the advancement of aeronautics and space science. The NASA Scientific and Technical Information (STI) program plays a key part in helping NASA maintain this important role.

The NASA STI Program operates under the auspices of the Agency Chief Information Officer. It collects, organizes, provides for archiving, and disseminates NASA's STI. The NASA STI program provides access to the NASA Aeronautics and Space Database and its public interface, the NASA Technical Reports Server, thus providing one of the largest collections of aeronautical and space science STI in the world. Results are published in both non-NASA channels and by NASA in the NASA STI Report Series, which includes the following report types:

- TECHNICAL PUBLICATION. Reports of completed research or a major significant phase of research that present the results of NASA programs and include extensive data or theoretical analysis. Includes compilations of significant scientific and technical data and information deemed to be of continuing reference value. NASA counterpart of peer-reviewed formal professional papers but has less stringent limitations on manuscript length and extent of graphic presentations.

- TECHNICAL MEMORANDUM. Scientific and technical findings that are preliminary or of specialized interest, e.g., quick release reports, working papers, and bibliographies that contain minimal annotation. Does not contain extensive analysis.

- CONTRACTOR REPORT. Scientific and technical findings by NASA-sponsored contractors and grantees.

- CONFERENCE PUBLICATION. Collected papers from scientific and technical conferences, symposia, seminars, or other meetings sponsored or cosponsored by NASA.

- SPECIAL PUBLICATION. Scientific, technical, or historical information from NASA programs, projects, and missions, often concerned with subjects having substantial public interest.

- TECHNICAL TRANSLATION. English-language translations of foreign scientific and technical material pertinent to NASA's mission.

Specialized services also include creating custom thesauri, building customized databases, organizing and publishing research results.

For more information about the NASA STI program, see the following:

- Access the NASA STI program home page at *http://www.sti.nasa.gov*

- E-mail your question via the Internet to *help@sti.nasa.gov*

- Fax your question to the NASA STI Help Desk at 301–621–0134

- Telephone the NASA STI Help Desk at 301–621–0390

- Write to:
  NASA Center for AeroSpace Information (CASI)
  7115 Standard Drive
  Hanover, MD 21076–1320

NASA/TM—2008-215176

Gas Foil Bearing Misalignment and Unbalance Effects

Samuel A. Howard
Glenn Research Center, Cleveland, Ohio

National Aeronautics and
Space Administration

Glenn Research Center
Cleveland, Ohio 44135

May 2008

This report is a formal draft or working paper, intended to solicit comments and ideas from a technical peer group.

This report contains preliminary findings, subject to revision as analysis proceeds.

Level of Review: This material has been technically reviewed by technical management.

Available from

NASA Center for Aerospace Information
7115 Standard Drive
Hanover, MD 21076–1320

National Technical Information Service
5285 Port Royal Road
Springfield, VA 22161

Available electronically at http://gltrs.grc.nasa.gov

Gas Foil Bearing Misalignment and Unbalance Effects

Samuel A. Howard
National Aeronautics and Space Administration
Glenn Research Center
Cleveland, Ohio 44135

Abstract

The future of U.S. space exploration includes plans to conduct science missions aboard space vehicles, return humans to the Moon, and place humans on Mars. All of these endeavors are of long duration, and require high amounts of electrical power for propulsion, life support, mission operations, etc. One potential source of electrical power of sufficient magnitude and duration is a nuclear-fission-based system. The system architecture would consist of a nuclear reactor heat source with the resulting thermal energy converted to electrical energy through a dynamic power conversion and heat rejection system.

Various types of power conversion systems can be utilized, but the Closed Brayton Cycle (CBC) turboalternator is one of the leading candidates. In the CBC, an inert gas heated by the reactor drives a turboalternator, rejects excess heat to space through a heat exchanger, and returns to the reactor in a closed loop configuration. The use of the CBC for space power and propulsion is described in more detail in the literature (Mason, 2003).

In the CBC system just described, the process fluid is a high pressure inert gas such as argon, krypton, or a helium-xenon mixture. Due to the closed loop nature of the system and the associated potential for damage to components in the system, contamination of the working fluid is intolerable. Since a potential source of contamination is the lubricant used in conventional turbomachinery bearings, Gas Foil Bearings (GFB) have high potential for the rotor support system. GFBs are compliant, hydrodynamic journal and thrust bearings that use a gas, such as the CBC working fluid, as their lubricant. Thus, GFBs eliminate the possibility of contamination due to lubricant leaks into the closed loop system.

Gas foil bearings are currently used in many commercial applications, both terrestrial and aerospace. Aircraft Air Cycle Machines (ACMs) and ground-based microturbines have demonstrated histories of successful long-term operation using GFBs (Heshmat et al., 2000). Small aircraft propulsion engines, helicopter gas turbines, and high-speed electric motors are potential future applications.

Nomenclature

C Bearing clearance, mm (in.)
L Bearing length, mm (in.)
N Rotor speed, rpm
W Rotor mass, g
m_r Residual unbalance magnitude, g-mm

Technology Background

GFBs (fig. 1) consist of an outer sleeve lined with a series of nickel-based superalloy sheet metal foils. The innermost sheet metal foil, or top foil, is smooth and constitutes the bearing inner surface against which the rotating shaft operates. The top foil is supported by a compliant structure, often made up of a layer of corrugated sheet metal foil referred to as bump foils, whose bumps behave like springs (Heshmat, 2000). It is presumed the bump foil layer gives the bearing flexibility that allows it to tolerate significant amounts of misalignment, and distortion that would otherwise cause a rigid bearing to fail. In addition, micro-sliding between the top foil and bump foil and the bump foil and the housing generates Coulomb damping which can increase the dynamic stability of the rotor-bearing system (Heshmat, 1994).

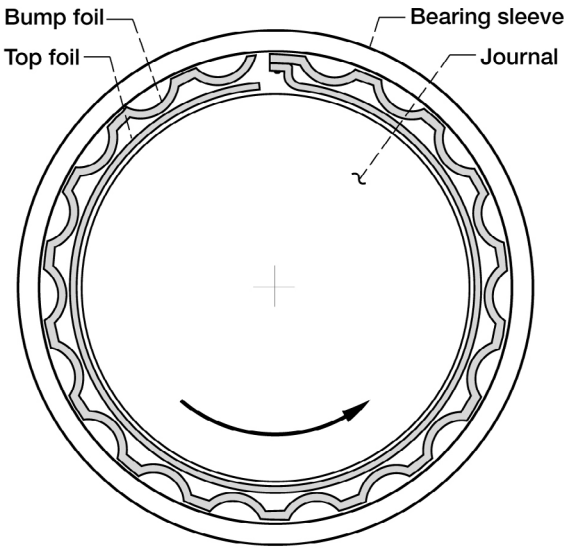

Figure 1.—Gas foil bearing schematic.

Though not as common, other designs exist to achieve an elastic foundation for the compliant top foil, such as overlapping leaves, cantilevered springs, and others.

During normal operation of a foil bearing supported machine, the rotation of the rotor generates a pressurized gas film that "pushes" the top foil out radially and separates the top foil from the surface of the rotating shaft. The pressure in the gas film is proportional to the relative surface velocity between the rotor and the foil bearing top foil. Thus, the faster the rotor rotates, the higher the pressure, and the more load the bearing can support. When the rotor first begins to rotate, the top foil and the rotor surface are in contact until the speed increases to a point where the pressure in the gas film is sufficient to push the top foil away from the rotor, and support its weight. Likewise, when the rotor slows down to a point where the speed is insufficient to support the rotor weight, the top foil and rotor again come in contact. Therefore, during start-up and shut down, a solid lubricant coating is used, either on the shaft surface or the foil, to reduce wear and friction (DellaCorte, 1998).

The tolerance to misalignment mentioned above is as yet an unknown for GFBs. Manufacturers claim GFBs can handle large misalignment due to the flexible nature of the inner bearing surface, but there is no experimental and little analytical verification of this capability. Unbalance effects are also a concern to designers. In an effort to address these concerns, the effects of both misalignment and unbalance are investigated experimentally in the current work.

Misalignment

An important issue for all turbomachinery, and therefore applicable to CBC space power systems is the degree of misalignment that a rotor bearing system can tolerate. The limits on misalignment dictate how precisely housings must be manufactured and how much thermal distortion can be tolerated. GFBs have been touted as having the ability to handle high degrees of misalignment relative to other bearing types, thus making them easier to integrate into high speed, high temperature applications. However, very little work has been reported on GFB misalignment. Carpino (1994) analyzed misalignment effects and found that load capacity is not affected strongly, but minimum film thickness decreases with increased misalignment. Those results were for very small angular misalignments (maximum angle equal to C/L radians) relative to those in the present tests (maximum angle approximately 10 times larger, assuming a clearance on the order of 25 μm), yet make clear a concern associated with misalignment. The viscous losses in the bearing, which lead to power loss and heat generation, are proportional to the viscosity of the

gas, and the wall shear stress of the fluid film (which varies inversely with the gas film thickness). Therefore, smaller minimum film thickness leads to higher power loss and greater heat generation.

Since the bearings presently used in the class of machines for which GFBs are considered as replacements are typically angular contact ball bearings, it is appropriate to compare the misalignment tolerance of the two. The amount of misalignment ball bearings can tolerate depends on the size, load, speed, and required life, but according to Zaretsky (1992), a typical allowable maximum angle of misalignment for angular contact ball bearings is 3.0×10^{-4} radians. The maximum angle can be related to a linear misalignment of bearing centers if the spacing between bearings is known. A test program was instigated to quantify the level of misalignment GFBs can tolerate for comparison and to help guide future oil-free turbomachinery design programs including space power systems.

The rotordynamic simulator test rig at the NASA Glenn Research Center (fig. 2) (Howard, 2007) was used to conduct misalignment tests on two 50.8 mm (2.00 in.) diameter journal GFBs. The rotordynamic simulator rig is an air turbine driven test rig that features completely oil-free operation. There are two journal GFBs near opposite ends of the rotor with two disks (a turbine and thrust bearing runner) mounted between the two journal bearings. In the configuration shown, the rotor weighs approximately 31 *N* (7.0 lb) and is roughly symmetric such that each journal bearing supports half the rotor weight. The journal bearings are housed in independent structures that can be moved relative to each other in transverse and angular directions. The independent bearing supports allow the operator to impose a known misalignment on the two journal bearings using a laser based alignment system that attaches to each bearing structure.

For the initial series of tests described here, one bearing structure was held fixed while the other was sequentially moved a small amount laterally (0.127 mm for each test) imposing a misalignment to both bearings until a failure was observed. Two physical quantities were measured during the tests, temperature and coast down time. The temperature was measured using thermocouples mounted to the underside of the bearing top foil close to the edge, 90° from top dead center in both directions, and at both ends for a total of 8 thermocouples, 4 on each bearing (fig. 3). Each test was run until the temperatures at a given test condition stabilized, indicating steady state operation. Data was collected for 20,000 rpm and

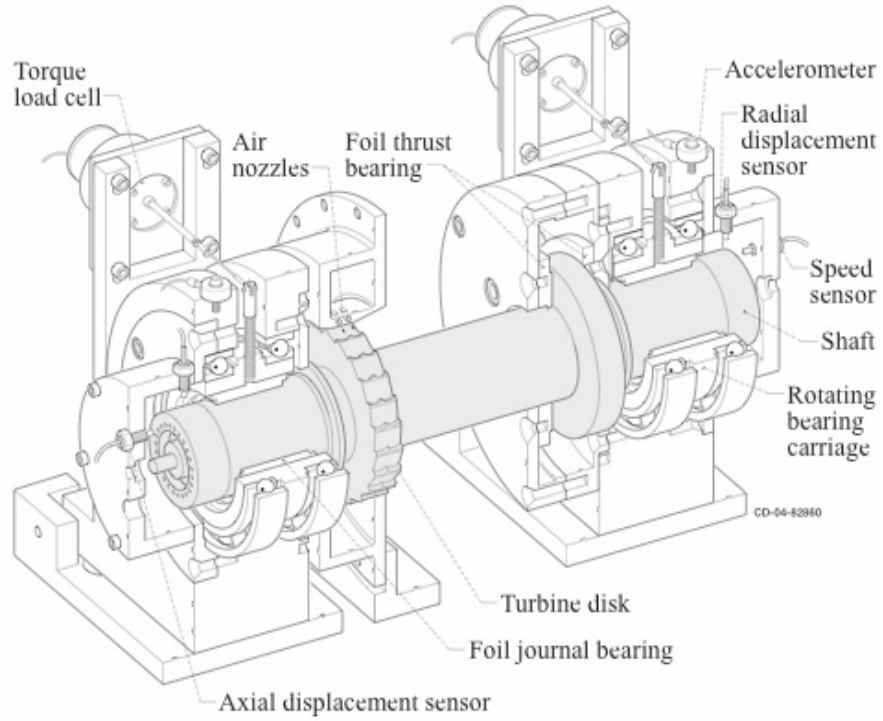

Figure 2.—Cut-away view of the rotordynamic simulator test rig.

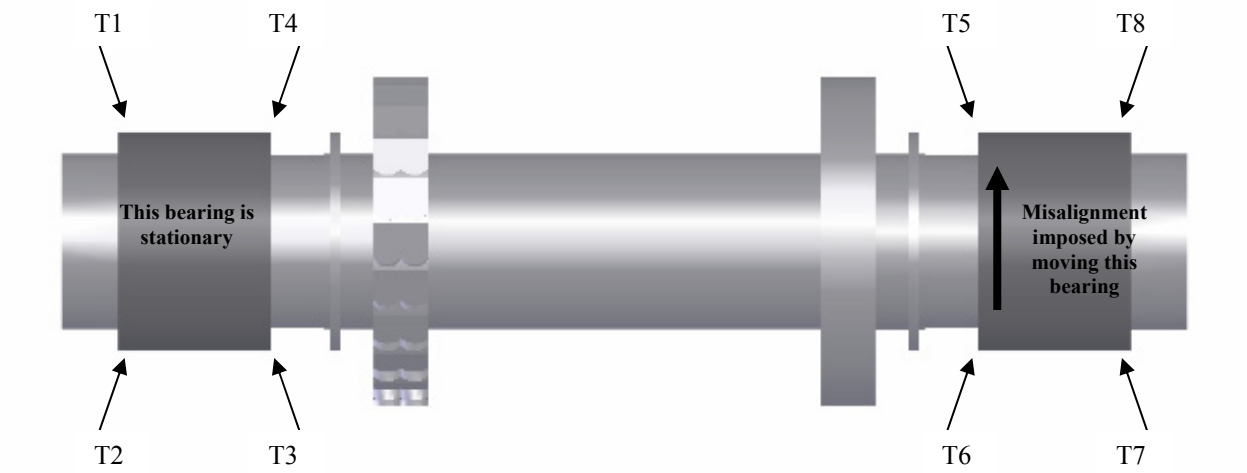

Figure 3.—Top view of rotordynamic simulator test rig showing thermocouple locations and misalignment direction.

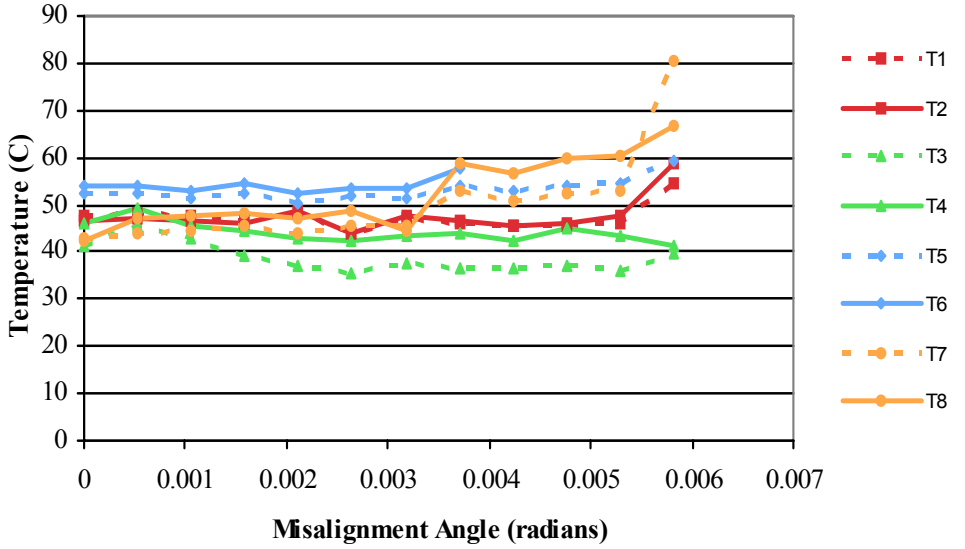

Figure 4.—Journal bearing edge temperatures at 20,000 rpm.

30,000 rpm. The expected result was to see overall higher temperatures and higher temperature gradients between opposite sides of the bearings (T2 versus T1 for example) at higher misalignment levels. The other observed quantity, coast down time was used as an indirect measure of bearing torque. It was anticipated that as the level of misalignment increased, the coast down time would decrease due to higher bearing losses.

Misalignment Results

Figure 4 shows the temperature data for steady operation at 20,000 rpm. In general, there is an upward trend on temperature with higher misalignment, as anticipated. The 30,000 rpm data, omitted here for brevity, shows the same trends with higher overall temperatures. The exceptions to the trend are T3 and T4. One possible cause of the downward trend in T3 and T4 is their proximity to the turbine, seen in figure 3. Since T3 and T4 are adjacent to the turbine, they are affected by the temperature of the turbine outlet flow. The turbine is driven by compressed air, and as the air expands through the nozzle, it cools. At higher misalignment, more flow is required to counteract the higher torque, resulting in more turbine exhaust. The increased turbine exhaust may cool the bearing in the location where T3 and T4 are mounted.

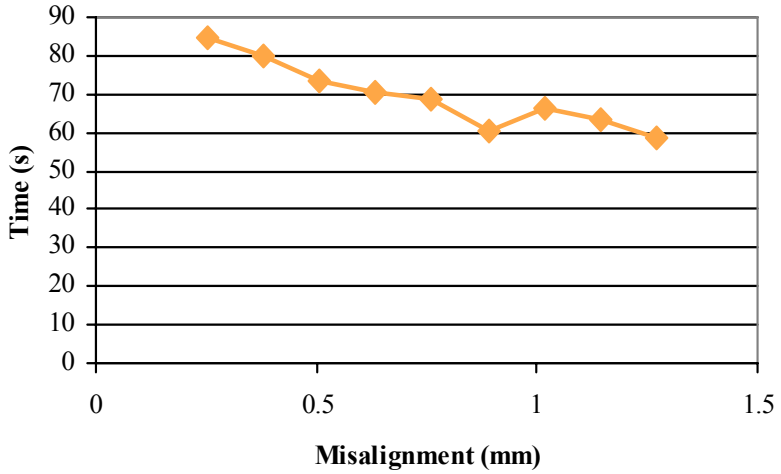

Figure 5.—Coast down time as a function of misalignment.

When the GFBs are misaligned, the bearings become more and more edge-loaded. The thermocouples were placed on the bearing in such a way to try to see the effect of the edge-loading in the form of increased temperature. For example, as the right hand bearing in figure 3 is moved upward in the picture, the film thickness near thermocouples T2, T4, T6, and T8 decreases, while at T1, T3, T5, and T7 it increases. Because thinner films are associated with higher heat generation, T2 should be hotter than T1, T4 hotter than T3, T6 hotter than T5, and T8 hotter than T7. In general, this result is observed. It should be noted that thermocouple T6 was damaged while increasing the misalignment after the run at 3.7×10^{-3} radians of misalignment, so there is no data for T6 beyond that test. Up to that point, it was behaving as expected.

Figure 5 shows the coast down time data as a function of misalignment. This data was not collected for the aligned case and the smallest misalignment case, but the trend shows that there is a general decrease in the time it takes to coast to a stop from 25,000 rpm as the misalignment increases. The decrease in coast down time can be attributed to increased power loss, or torque in the bearings. Modifications are planned for the rig to enable direct torque measurements in the future.

At a maximum misalignment of 5.8×10^{-3} radians (1.4 mm/0.055 in. over 240mm/9.5 in.) and 20,000 rpm, a failure was experienced and testing was stopped. GFBs can fail in several ways (Dykas and Howard, 2004, Radil, et al., 2002), but this failure was a typical failure that is seen when load capacity is reached. The torque in the bearings increases rapidly, accompanied by an increase in temperature with no increase in speed or load. At the onset of the failure, it was observed that more turbine pressure was needed to maintain the same speed. As the failure progressed, more turbine pressure could not overcome the increase in torque, and speed decreased even with more pressure. When this occurred, the test was stopped.

It was determined that for the configuration of the rotordynamic simulator test rig, 5.8×10^{-3} radians is the limit of misalignment that the GFBs can sustain. From the failure mode, it is reasonable to assume that the load capacity of the bearings decreased with increased misalignment until the load capacity fell below the weight of the rotor, and failure was observed. It appears then, that the amount of misalignment a GFB can tolerate is likely a function of how much load it is supporting in relation to its load capacity.

In the case studied here, the maximum misalignment angle obtained, 0.0058 radians, is nearly 20 times the amount tolerable with angular contact ball bearings. The advantage over radial ball bearings and cylindrical roller bearings is less at 2 and 6 times, respectively, but still significant.

Unbalance Effects

Design and integration of gas foil bearing supported turbomachinery suffers from a lack of understanding and design tools to accurately predict rotordynamic behavior. The lack of design tools can be attributed in part, to the complexity of analytically modeling gas foil bearings to calculate traditional bearing force coefficients. The bearing stiffness and damping coefficients, to a great degree, dictate the dynamic behavior of the rotor/bearing system. The difficulty of modeling GFBs analytically stems from the interaction of the fluid film and the structural compliance in the bearings themselves. While analytic models do exist, Carpino and Talmadge (2006) present the most current and advanced model, few have been experimentally validated to date.

Experimental measurements of GFB force coefficients is also lacking in sufficient quantity to offer machine designers the necessary information to conduct reasonable detailed designs. Howard, et al. (2001) reported trends in bearing rotordynamic properties with increased temperature, but absolute measurement of coefficients was not possible with the test set-up. In order to advance the understanding of GFB rotordynamic coefficients, NASA Glenn Research Center has modified the same test rig used in the above misalignment tests to enable force coefficient estimation from measured unbalance effects.

The rotordynamic simulator test rig was modified by adding a series of threaded holes at each end of the rotor to accept unbalance masses in the form of small set screws. In this manner, a set screw of known mass can be added to a threaded hole of know angular position to cause a known change in the rotor balance condition. The resulting unbalance response is measured by a set of four displacement sensors, two at each end of the rotor, 90° apart.

The purpose of the present tests, is to observe the effect of increased levels of unbalance on the rotor/bearing system. To begin the unbalance tests, the rotor was balanced in two planes using a horizontal hard bearing balancing machine at the NASA Glenn Research Center. The total residual unbalance after the balancing procedure was 1.482 g-mm (0.00204 oz-in.). The distribution of unbalance at each end of the rotor, and the angle relative to a key-phaser reference point (defined as 0°) on the rotor is given in table 1.

TABLE 1.—RESIDUAL UNBALANCE MASS DISTRIBUTION

Axial location	Mass, g	Radius, mm	Unbalance magnitude, g-mm	Mass, μoz_m	Radius, in.	Unbalance magnitude, oz_m-in.	Angle, deg
Compressor end	0.0276	31.75	0.876	971	1.25	0.00121	135
Turbine end	0.0191	31.75	0.606	668	1.25	0.000835	90

Using industry standards (ISO 1940-1:2003), the allowable residual unbalance for machines of this class (grade G2.5) can be approximated by the following:

$$m_r \le 23.2W(g)/N(rpm)$$
$$m_r \le 1.50g - mm$$

With a weight of 3.18 kg and maximum speed of 50,000 rpm, the unbalance should be 1.50 g-mm (0.00208 oz-in.) or less (total, assuming half at each end of the rotor). The residual unbalance of this rotor is within the above limit, although it is slightly higher than desired at the compressor end and slightly lower than necessary at the turbine end. Since the objective here is to observe the effect of unbalance over a large range, this condition is considered the balanced case, and is used as a baseline to which other unbalance conditions are compared. The smallest weight that can reasonably be added in the form of a set screw is approximately 0.0220 g (775 μoz.) and is added to the rotor at a radius of 18.4 mm (0.725 in.) at the extreme ends of the rotor. The test procedure consists of sequentially adding weights in increments of 0.0220 g (775 μoz.) until a sufficiently high level of unbalance is reached and comparing the results to the baseline. Table 2 lists all the tests and the corresponding masses added with their location and angle.

TABLE 2.—INTENTIONALLY ADDED UNBALANCE MASS DISTRIBUTION

Test number	Axial location	Mass, g	Radius, mm	Unbalance magnitude, g-mm	Mass, μoz_m	Radius, in.	Unbalance magnitude, oz_m-in.	Angle, deg
1	Compressor end	0.0210	18.42	0.387	740	0.725	0.000536	135
	Turbine end	0.0210	18.42	0.387	740	0.725	0.000536	90
2	Compressor end	0.0440	18.42	0.811	1550	0.725	0.00112	135
	Turbine end	0.0440	18.42	0.811	1550	0.725	0.00112	90
3	Compressor end	0.0660	18.42	1.216	2330	0.725	0.00169	135
	Turbine end	0.0655	18.42	1.207	2310	0.725	0.00167	90
4	Compressor end	0.0880	18.42	1.621	3100	0.725	0.00225	135
	Turbine end	0.0880	18.42	1.621	3100	0.725	0.00225	90
5	Compressor end	0.110	18.42	2.026	3880	0.725	0.00281	135
	Turbine end	0.110	18.42	2.026	3880	0.725	0.00281	90
6	Compressor end	0.132	18.42	2.431	4650	0.725	0.00337	135
	Turbine end	0.132	18.42	2.431	4650	0.725	0.00337	90
7	Compressor end	0.210	18.42	3.868	7400	0.725	0.00536	135
	Turbine end	0.210	18.42	3.868	7400	0.725	0.00536	90

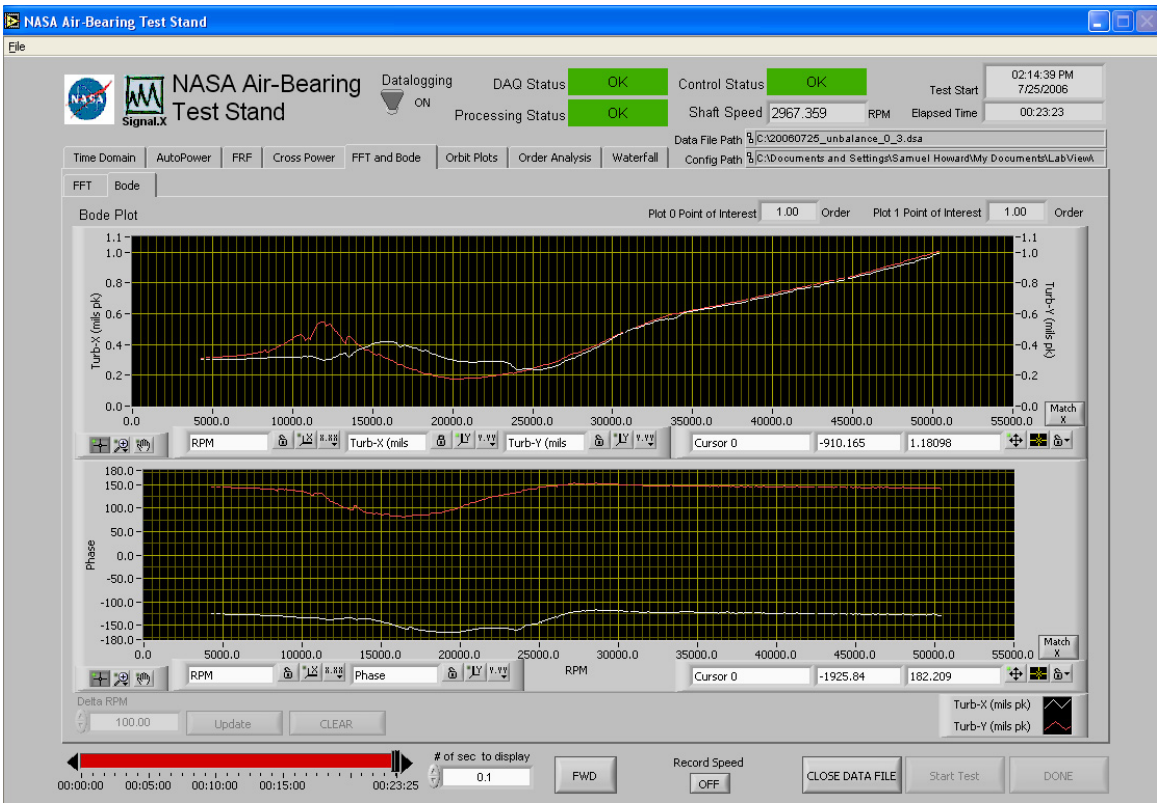

Figure 6.—Baseline Bode plot with no added unbalance mass.

Unbalance Results

Figure 6 shows a Bode plot of the baseline unbalance condition at the turbine end of the rotor. The Bode plot is a graphical representation of the synchronous vibration amplitude and phase as a function of speed. Physically, it represents the component of the vibration that can usually be attributed to unbalance. Because unbalance forces rotate with the rotor at the same frequency that the rotor spins, they cause vibrations at that same frequency. By using a tracking filter whose frequency follows the running speed of

the rotor, one can identify the unbalance response within the broad-spectrum vibration signal. Critical speeds in the rotor system are often visible on Bode plots as peaks in the vibration amplitude accompanied by a phase shift. Theoretically, the phase should change by 180° as a critical speed is traversed, but in reality the phase shift is often much different from 180° for various reasons. In figure 6, two apparent critical speeds can be seen, one on the Turb-X plot (white) and one on the Turb-Y plot (red). The two lines represent the horizontal and vertical responses (Turb-X and Turb-Y respectively). These two critical speeds are commonly referred to as the rigid body modes because they have mode shapes that contain very little to no shaft bending, the shaft vibrates as a rigid body. One can see from the figure that the lowest frequency critical speed occurs at approximately 13,500 rpm, and contains mostly vertical motion at the measurement location (close to the bearing) as there is a peak in the response of the Y-axis vibration with no corresponding X-axis peak. The second critical speed occurs near 17,000 rpm and contains mostly horizontal motion at the bearing. Above the second critical speed, the response grows steadily with speed. This growth is due to the rotor approaching the third critical speed, which is beyond the speed range of the test. The third critical speed for this rotor is the first bending mode, so called because its mode shape involves significant bending of the shaft. The purpose of these tests is to add unbalance and observe the corresponding changes in the unbalance response, or Bode plot.

The following four figures (7 to 10) are a succession of Bode plots taken with increasing levels of unbalance from 0.811 g-mm up to 3.87 g-mm (112 to 536 μoz-in.). In the interest of conserving space, not all of the Bode plots generated are shown. The plots shown are from the baseline "balanced" case, and from tests 2, 4, 6, and 7 since they are adequate to visualize the trends. As mentioned above, adding unbalance was accomplished by inserting set screws in threaded holes in the ends of the rotor. The intention was to add mass in increments of 0.0220 g (775 μoz.) at the same angular positions as the residual unbalance. The mass of the set screws is controlled by filing a large set screw to the appropriate length to get the desired mass. Since the filing process was done manually, the mass added in each test was not precisely 0.0220 g (775 μoz.). However, each set screw was weighed and the precise mass added was noted for each test (table 2). The maximum amount of unbalance tested was 3.87 g-mm (0.00536 oz-in.) at each end, which combined with the residual unbalance resulted in a total unbalance condition of nearly an order of magnitude greater than the ISO standard. Since the magnitudes of vibration were high, and trends could be seen at this point, no larger unbalance conditions were attempted.

Figures 7 to 10 show the trends observed as the unbalance increases. The critical speed at 13,500 rpm in the baseline case increased in frequency up to 16,000 rpm while the magnitude decreased from 12.7 μm (0.0005 in.) peak to just under 10 μm (0.00040 in.) peak. Similarly, the critical speed at 17,000 rpm increased in frequency to 19,000 rpm and decreased in magnitude from roughly 10 μm (0.00041 in.) to 8.9 μm (0.00035 in.).

These results might seem surprising at first. Linear bearing assumptions commonly used in rotordynamic calculations would predict that an increase in unbalance would result in proportionally higher vibration amplitudes, and critical speeds would remain fixed. However, the present results support the idea that gas foil journal bearing force coefficients are non-linear. As the unbalance force increases, the GFB stiffness increases resulting in higher critical speeds and lower vibration amplitudes. This effect would be impossible to predict using linear bearing properties, and illustrates the importance of rotordynamic simulator testing to augment computational rotordynamic analysis in the design phase of advanced oil-free turbomachinery.

Some other important points to observe from the unbalance response plots are the damping capabilities of GFBs and the relatively high amplitude vibration tolerance. The stability of rotor/bearing systems is an important consideration in the design of high speed, lightly loaded turbomachinery such as space power generation systems. With that in mind, it is useful to notice the shape of the critical speed peaks on the above Bode plots. The width of the vibration peak on the Bode plot is an indication of the amount of damping in the system. The wider the peak, the more damped the natural frequency, and conversely, the narrower the peak, the less damped the natural frequency. Thus, the appearance of wide,

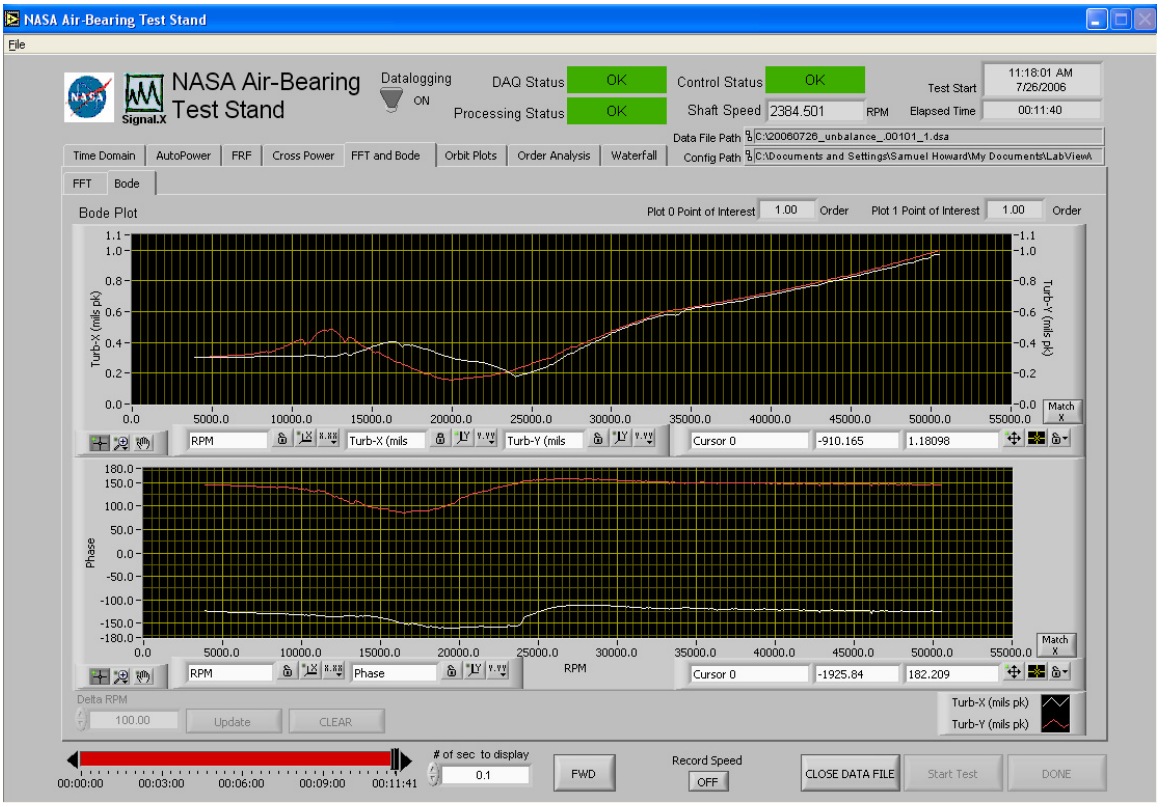

Figure 7.—Bode plot with 0.811 g-mm unbalance added at each end from test number 2.

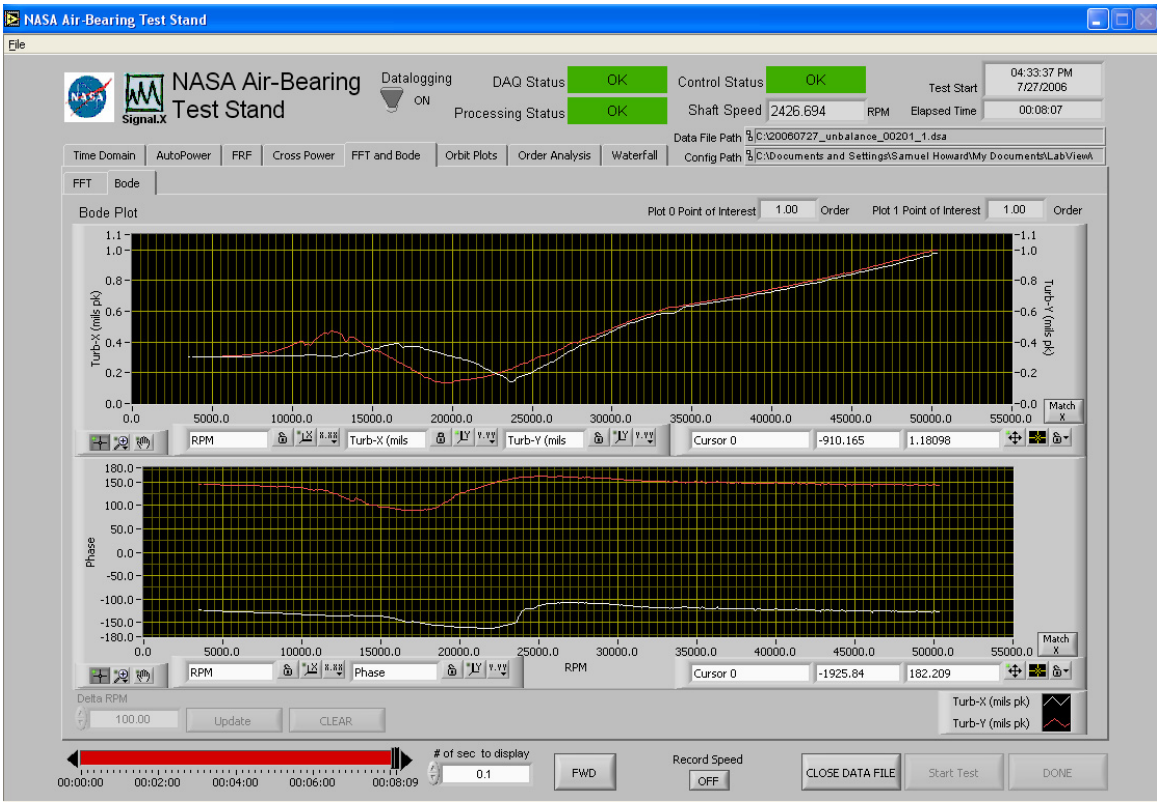

Figure 8.—Bode plot with 1.621 g-mm unbalance added at each end from test number 4.

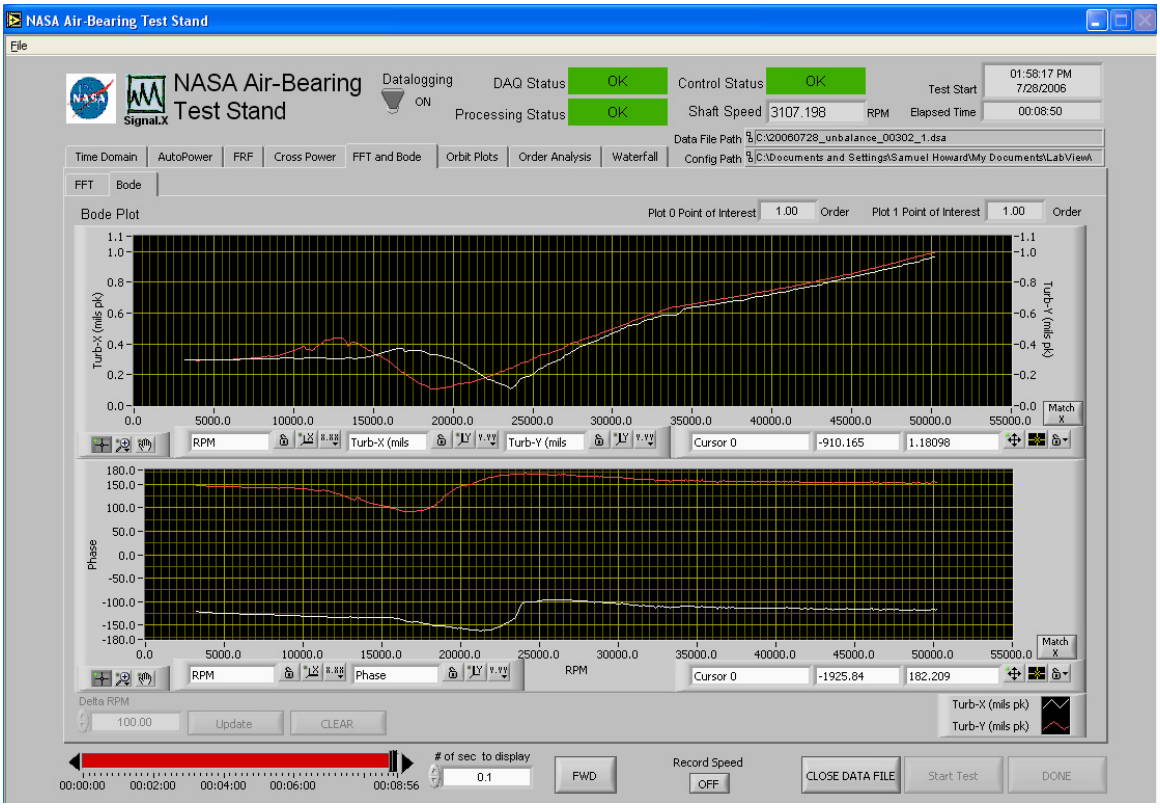

Figure 9.—Bode plot with 2.431 g-mm unbalance added at each end from test number 6.

Figure 10.—Bode plot with 3.868 g-mm unbalance added at each end from test number 7.

low amplitude critical speed peaks indicates that the natural frequencies of this system are well damped, and likely present less of a concern for stability at high speed. In fact, the ability to operate to at least 50,000 rpm further supports this claim.

The amplitude of vibration in these plots is rather high. The cause of the high amplitude is believed to be large clearances in the GFBs. Previous GFB work (Radil, et al., 2002, DellaCorte, et al., 2006) has shown that tighter bearings result in more control over rotor vibrations, but the increased control comes at the cost of higher power loss and thermal management requirements. There is a trade-off between vibration amplitude and thermal stability. The bearings used in these tests are relatively loose and therefore result in high vibration amplitudes. The industry standard for acceptable vibration amplitude is up to approximately 3.8 μm (0.00015 in.) peak-to-peak at 13,000 rpm and falls to 2.5 μm (0.0001 in.) peak to peak at 50,000 rpm (ISO 10816-1:1994). The maximum vibration amplitude of the test rotor at 13,000 rpm is 28 μm (0.0011 in.), and 50 μm (0.002 in.) at 50,000 rpm. These vibration amplitudes, as high as 20 times the industry standard, are unacceptable for a machine put into service, but the successful operation of the test rig with such high vibration is an indication of the robustness of GFBs to handle extreme operating conditions, at least in a laboratory environment for short duration.

Conclusions

Misalignment and unbalance effects on a gas foil bearing supported rotor have been presented. Misalignment of two coaxial journal bearings has the expected result of increased temperature at the edges of the bearings, and increased torque observed as a decrease in coast down time. The ability of GFBs to handle high degrees of misalignment were verified. Successful operation was achieved with misalignments of 20, 6, and 2 times the acceptable level for angular contact ball, cylindrical roller, and radial ball bearings, respectively.

The effect of unbalance on the operation of a simulated rotor was also presented. Unbalance masses were added to a rotor supported on gas foil journal bearings and the resulting synchronous vibration amplitude was measured. Results imply that increased unbalance forces result in higher bearing stiffness. The higher bearing stiffness forces the natural frequencies of the rotor system up, and the vibration amplitudes down. This result is in opposition to a linear bearing assumption, and supports the need for advanced analytical models coupled with rotor simulator testing for successful GFB integration into advanced turbomachinery. Based upon these tests, with high tolerance to misalignment, and ability to sustain large unbalance levels, GFBs represent an excellent enabling technology for long-life, oil-free turbomachinery power conversion systems.

References

1. Carpino, M., Peng, J.P., and Medvetz, L., “Misalignment in a Complete Shell Gas Foil Journal Bearing,” *Tribology Transactions*, vol. 37, no. 4, 1994, pp. 829–835.
2. Carpino, M., and Talmadge, G., “Prediction of Rotor Dynamic Coefficients in Gas Lubricated Foil Journal Bearings with Corrugated Sub-Foils,” *Tribology Transactions*, vol. 49, 2006, pp. 400–409.
3. DellaCorte, C., “The Evaluation of a Modified Chrome Oxide Based High Temperature Solid Lubricant Coating for Foil Gas Bearings,” NASA/TM—1998-208660, 1998.
4. DellaCorte, C., Radil, K.C., Bruckner, R.J., and Howard, S.A., “A Preliminary Foil Gas Bearing Performance Map,” NASA/TM—2006-214343, 2006.
5. Dykas, B.D., and Howard, S.A., “Journal Design Considerations for Turbomachine Shafts Supported on Foil Air Bearings,” *Tribology Transactions*, vol. 47, no. 4, 2004, pp. 508–516.
6. Heshmat, H., “Advancements in the Performance of Aerodynamic Foil Journal Bearings: High Speed and Load Capability,” *Transactions of the ASME J. of Tribology*, 116, 1994, pp. 287–295.
7. Heshmat, H., “High load capacity compliant foil hydrodynamic journal bearing,” U.S. Patent 6,158,893, 2000.

8. Heshmat, H., Walton, J.F., DellaCorte, C., and Valco, M.J., "Oil-Free Turbocharger Demonstration Paves the Way to Gas Turbine Engine Applications," presented at the *ASME/IGTI*, Munich, Germany, ASME paper number 2000–GT–620, 2000.
9. Howard, S.A., "A New High-Speed Oil-Free Turbine Engine Rotordynamic Simulator Test Rig," NASA/TM—2007-214489, 2007.
10. Howard, S.A., DellaCorte, C., Valco, M.J., Prahl, J.M., and Heshmat, H., "Dynamic Stiffness and Damping Characteristics of a High-Temperature Air Foil Journal Bearing," *Tribology Transactions*, vol. 44, no. 4, 2001, pp. 657–663.
11. Mason, L.S., "A Power Conversion Concept for the Jupiter Icy Moons Orbiter," *1st AIAA/ASME/IEEE International Energy Conversion Engineering Conference*, Portsmouth, Virginia, August 17–21, 2003, AIAA–2003–6007.
12. Radil, K.C., Howard, S.A., and Dykas, B.D., "The Role of Radial Clearance on the Performance of Foil Air Bearings," NASA/TM—2002-211705, 2002.
13. Zaretsky, E.V., *Life Factors for Rolling Bearings*, Society of Tribologists and Lubrication Engineers, Park Ridge, IL, 1992, pp. 145–158.

REPORT DOCUMENTATION PAGE	Form Approved OMB No. 0704-0188

1. REPORT DATE *(DD-MM-YYYY)*	2. REPORT TYPE	3. DATES COVERED *(From - To)*
01-05-2008	Technical Memorandum	

4. TITLE AND SUBTITLE
Gas Foil Bearing Misalignment and Unbalance Effects

5a. CONTRACT NUMBER

5b. GRANT NUMBER

5c. PROGRAM ELEMENT NUMBER

6. AUTHOR(S)
Howard, Samuel, A.

5d. PROJECT NUMBER

5e. TASK NUMBER

5f. WORK UNIT NUMBER
WBS 877868.02.07.03.01.01

7. PERFORMING ORGANIZATION NAME(S) AND ADDRESS(ES)
National Aeronautics and Space Administration
John H. Glenn Research Center at Lewis Field
Cleveland, Ohio 44135-3191

8. PERFORMING ORGANIZATION REPORT NUMBER
E-16419

9. SPONSORING/MONITORING AGENCY NAME(S) AND ADDRESS(ES)
National Aeronautics and Space Administration
Washington, DC 20546-0001

10. SPONSORING/MONITORS ACRONYM(S)
NASA

11. SPONSORING/MONITORING REPORT NUMBER
NASA/TM-2008-215176

12. DISTRIBUTION/AVAILABILITY STATEMENT
Unclassified-Unlimited
Subject Category: 37
Available electronically at http://gltrs.grc.nasa.gov
This publication is available from the NASA Center for AeroSpace Information, 301-621-0390

13. SUPPLEMENTARY NOTES

14. ABSTRACT
The effects of misalignment and unbalance on gas foil bearings are presented.

15. SUBJECT TERMS
Gas bearings; Foil bearings; Rotor dynamics; Turbomachinery

16. SECURITY CLASSIFICATION OF:			17. LIMITATION OF ABSTRACT	18. NUMBER OF PAGES	19a. NAME OF RESPONSIBLE PERSON
a. REPORT	b. ABSTRACT	c. THIS PAGE			STI Help Desk (email:help@sti.nasa.gov)
U	U	U	UU	18	19b. TELEPHONE NUMBER *(include area code)* 301-621-0390